



Top Quark Mass Measurement using Matrix Element Method and Lepton+Jets Channel

The CDF Collaboration

URL <http://www-cdf.fnal.gov>

(Dated: April 17, 2009)

We present a measurement of the top quark mass using $t\bar{t}$ candidate events for the lepton+jets decay channel. The top quark mass is extracted using the unbinned maximum likelihood method with the probability density function evaluated for each event using leading-order $t\bar{t}$ and W +jets matrix elements and a set of parameterized jet-to-parton-mapping functions. In addition to the top quark mass the likelihood function is maximized with respect to a jet energy scale correction, constrained *in situ* with the hadronic W boson mass, and an approximate fraction of the well reconstructed $t\bar{t}$ signal events in the candidate sample. We describe the method, present statistical and systematic uncertainties for 578 observed candidate events, corresponding to integrated luminosity of $3.2 fb^{-1}$ of $p\bar{p}$ collisions data collected with the Tevatron CDF II detector at Fermilab and requiring exactly one energetic lepton, large missing energy, exactly four energetic jets with absolute value of pseudo-rapidity less than two and with at least one of the jets identified as coming from a b-quark. We measure a top quark mass $m_t = [172.4 \pm 1.9] GeV/c^2$.

Preliminary Results for 2009 Conferences

I. INTRODUCTION

The top quark is the heaviest known fundamental particle. The top quark mass is an intrinsic parameter of the Standard Model and its precise measurement can therefore provide constraints on other parameters of the model, most pertinently the mass of the Higgs boson. It is important to measure the top quark mass in order to test and understand the Standard Model and its extensions.

In this note we present an updated measurement of the top quark mass using the matrix element analysis technique and the $t\bar{t}$ lepton+jets decay channel candidate events. The previous measurement using this technique resulted in $m_t = 170.8 \pm 2.2(stat + JES) \pm 1.4(syst) GeV$ and used $955 pb^{-1}$ of data [1]. This measurement uses CDF data between February 04 2002 and August 24 2008 corresponding to an integrated luminosity of $3.2 fb^{-1}$.

and measure the top quark mass $m_t = [172.4 \pm 1.9] GeV/c^2$.

II. SELECTION OF DATA AND MONTE CARLO SAMPLES

The CDF detector is described in detail in [2]. Our analysis requires all data and Monte Carlo events to pass criteria which include requiring:

- Exactly four well reconstructed jets with $|\eta|$ less than 2 and transverse energy E_T greater than $20 GeV$
- At least one of the jets is identified as coming from a b-quark, using Secondary Vertex tagging algorithm and fully operational Silicon Tracking detector.
- Exactly one well reconstructed high P_T lepton
- Missing transverse energy \cancel{E}_T is greater than $20 GeV$

All background events are simulated using Monte Carlo except for QCD, where events are taken from another data sample and have the same requirements for jets, but not for leptons.

For our analysis, we use CDF dataset which includes all data collected between Feb 04, 2002 and Aug 24, 2008 and represents approximately $3.2 fb^{-1}$ of data. We find a total of 578 candidate events passing our requirements for analysis.

Our signal MC samples are all Pythia [3] generated $t\bar{t}$ with various top quark masses. Our nominal sample has a mass of $175 GeV/c^2$. We use another 16 samples with masses ranging from 161 to $185 GeV/c^2$. Each of these samples has more than one million events. $W + jets$ and $Z + jets$ background Monte Carlo is generated using Alpgen plus Pythia. Diboson samples are generated with Pythia. Single top samples are generated with MadEvent + Pythia. Table I gives the expected number of signal and background events.

To test our event selection and background estimation, we have plotted several variables from our events. Figure 17 shows plots for some variables from our 578 selected candidate events compared to the expected distribution from our signal and background modeling. Many plots may be found on our public web page.

TABLE I: Number of expected signal and background events corresponding to the total integrated luminosity of $3.2 fb^{-1}$.

sample	# of events
$t\bar{t}$ signal	425.0 ± 58.9
$Wb\bar{b}$	39.0 ± 12.7
non- W	25.0 ± 20.5
$W + 4p$	22.5 ± 5.7
$Wc\bar{c}$	20.3 ± 6.7
Wc	10.7 ± 3.6
WW	4.2 ± 0.5
$Z + \text{light flavour}$	3.9 ± 0.5
single top (s-channel)	3.3 ± 0.3
single top (t-channel)	3.3 ± 0.3
WZ	1.5 ± 0.2
ZZ	0.4 ± 0.1
total	559.2 ± 67.0

III. MATRIX ELEMENT ANALYSIS TECHNIQUE

We extract the top quark mass using the *unbinned maximum likelihood method* with the likelihood function

$$\mathcal{L}(\alpha; \vec{x}) = \prod_{i=1}^N P(\vec{x}_i; \alpha), \quad (1)$$

where \vec{x} are the measured quantities in the sample of N candidate events and the likelihood parameters $\vec{\alpha}$ are the top quark mass, m_{top} ; the jet energy scale correction, Δ_{JES} , defined as the number of sigmas by which each jet is shifted from its measured value; and ν_{sig} , the approximate fraction of well reconstructed signal events in the candidates sample. Signal events are defined as events consistent with leading order production of $t\bar{t}$ pair decaying into the lepton + jets channel. The probability density function (p.d.f.), P , is calculated for each event in the final sample and contains p.d.f.'s describing the dominant physical processes contributing to the events in the likelihood. In the case of the lepton + jets decay channel, these processes are $t\bar{t}$ production and W + jets production, the dominant background. We make the approximation that these two processes fully describe each event in our final sample and are statistically independent from each other. We call them *signal* P_s and *background* P_b probabilities and form the event p.d.f. P as the linear combination

$$P(\vec{x}; m_t, \Delta_{JES}, \nu_{sig}) = \nu_{sig} P_s(\vec{x}; m_t, \Delta_{JES}) + (1 - \nu_{sig}) P_b(\vec{x}; \Delta_{JES}), \quad (2)$$

where the constraint $0 \leq \nu_{sig} \leq 1$ ensures the sum of the two normalized p.d.f.s is itself properly normalized. These p.d.f.s for the processes are defined in the kinematic phase-space of all possible measurements. Since in practice this phase-space is always limited by the physical properties of the detector apparatus and final sample selection, we introduce an overall *acceptance* function, $Acc(\vec{x})$, describing these effects. The acceptance is defined as the fraction of fully reconstructed events passing selection out of the total possible for a given set of measurable parameters (\vec{x}):

$$P'(\vec{x}; \alpha) = Acc(\vec{x}) P(\vec{x}; \alpha). \quad (3)$$

This acceptance is independent of the underlying process and is solely a property of the detector and selection procedure. It is also independent of the likelihood parameters and any overall constant (with respect to the parameters) factor in the product of Equation 1 has no effect on the outcome of the likelihood maximization. However this acceptance term contributes to the expression for the p.d.f. normalization integral $N(m_t, \Delta_{JES})$ as the mean acceptance, which does depend on the parameters of the likelihood.

The explicit expression for the logarithm of the likelihood function used in this analysis is given below:

$$\log \mathcal{L}(m_t, \Delta_{JES}, \nu_{sig}; \vec{x}) = - \sum_{i=1}^N \log \left[\nu_{sig} \frac{P_{t\bar{t}}(m_t, \Delta_{JES})}{\sigma(m_t) \overline{Acc}(m_t, \Delta_{JES})} + (1 - \nu_{sig}) \nu_{bkg} P_{W+jets} \right] \quad (4)$$

where N is the number of the candidate events in the final sample, $\sigma(m_t) \overline{Acc}(m_t, \Delta_{JES}) = N(m_t, \Delta_{JES})$ is the overall normalization for the signal p.d.f. and ν_{bkg} is the normalization term for the background p.d.f..

This function (Equation 4) is first maximized with respect to the approximate signal fraction ν_{sig} using MINUIT [5]. After taking the profile at maximum ν_{sig} our log likelihood function is calculated on a two dimensional grid. The top mass and the jet energy scale correction Δ_{JES} are then extracted using a two-dimensional fit to the likelihood function evaluated on the grid, and the statistical uncertainty associated with the measurement is described by the ellipse corresponding to a change of 0.5 from the parabola's maximum. Thus in our method the statistical errors are always symmetric.

The measured uncertainty, $\sigma_{m_t}^{measured}$, represents the overall statistical uncertainty on the top mass, and therefore must include the uncertainty associated with the measured Δ_{JES} . We therefore take $\sigma_{m_t}^{measured}$ along the major axis of the ellipse. Similarly, $\sigma_{\Delta_{JES}}^{measured}$ is also taken along the major axis of the ellipse.

It would be prohibitively difficult to parameterize $Acc(\vec{x})$ for all \vec{x} , but the mean acceptance $\overline{Acc}(m_t, \Delta_{JES})$ is independent of \vec{x} and can be easily extracted from our Monte Carlo:

$$\overline{Acc}(m_t, \Delta_{JES}) = \frac{N_{accepted}}{N_{generated}} \quad (5)$$

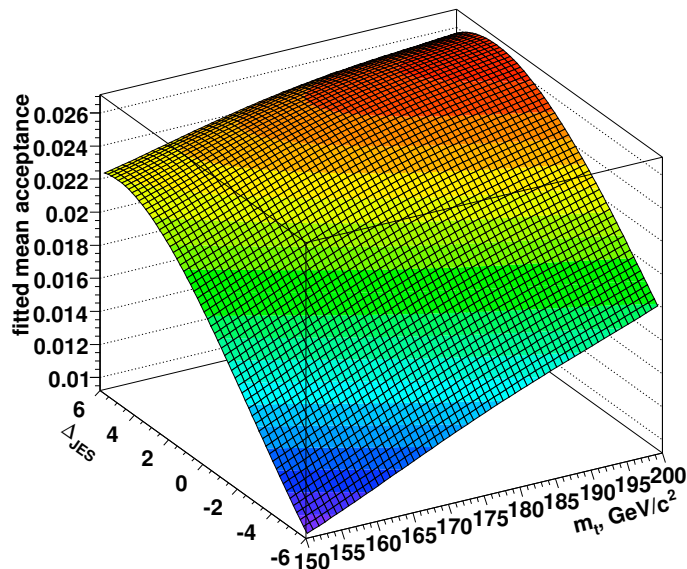


FIG. 1: Approximation function for the mean acceptance $\overline{Acc}(m_t, \Delta_{JES})$.

The simulated acceptance distribution is fitted to a 2D 4^{th} order polynomial (Figure 1) and that function is used in the measurement.

The event p.d.f. for a given physical scattering process is constructed by inputting measured quantities to its normalized parton-level differential cross-section and integrating over any unknown variables. Measured quantities (\vec{x}) are translated into parton level (\vec{y}) with the appropriate resolution using a *transfer function*.

In this analysis, we assume our detector does a good job of measuring all the components of the electron and muon momenta. Therefore, we consider the transfer function to be δ -functions for these quantities. However, our detector has significant resolution effects in jet energy. We parameterize the jet energy response of our detector with a *jet energy transfer function*, W , assuming the response is independent for each jet.

$W(E_p, E_j, \Delta_{JES}) = W(E_i^x, E_i^y, \Delta_{JES})$, is the probability of observing a jet with energy E_j when a parton with energy E_p is produced. It satisfies the normalization condition $\int W(E_j, E_p, \Delta_{JES}) dE_j = 1$, so that each parton produced corresponds to exactly one detected jet.

Our jet energy transfer function (ETF) is parameterized as a double Gaussian whose main variable is $\delta = E'_j - E_p$ - that is, this difference between the jet energy and the parton energy.

$$W(E'_j - E_p) = W(\delta) = \frac{1}{\sqrt{2\pi}(p_2 + |p_3|p_5)} \left[e^{-\frac{(\delta-p_1)^2}{2p_2^2}} + |p_3| \cdot e^{-\frac{(\delta-p_4)^2}{2p_5^2}} \right] \quad (6)$$

E'_j is the measured jet energy E_j adjusted with the floating Δ_{JES} . The energy transfer functions for light and b-quarks are shown in Figures 2 and 3.

In previous versions of this analysis the jet angles were assumed sufficiently well measured that their transfer functions could be approximated by Dirac delta functions. That approximation was found to be invalid in the case of the angle between the two hadronic W jets, α_{12} , and in fact the measurement of that angle was seen to cause a bias in the hadronic W boson mass. Since the method relies on an accurate measurement of the W mass for the in-situ Δ_{JES} calibration, it was important for us to introduce angular transfer functions (ATFs) to account for that effect. These ATFs are binned in $\cos(\alpha_{12})$, and are parameterized by a skew-Cauchy distribution plus two Gaussians using a fit to Pythia Monte-Carlo events (Figures 4 and 5). We also introduced a similar second set of ATFs to correct a similar bias observed in the angle between the hadronic W boson and b-quark, α_{Wb} , which affected the hadronic top quark mass.

Integration over the ATFs in $\cos(\alpha_{12})$ and $\cos(\alpha_{Wb})$ corrects the observed bias in the hadronic W boson and top quark masses, and also accounts for the angular resolution effects to which we are most sensitive (those that affect the W and top masses).

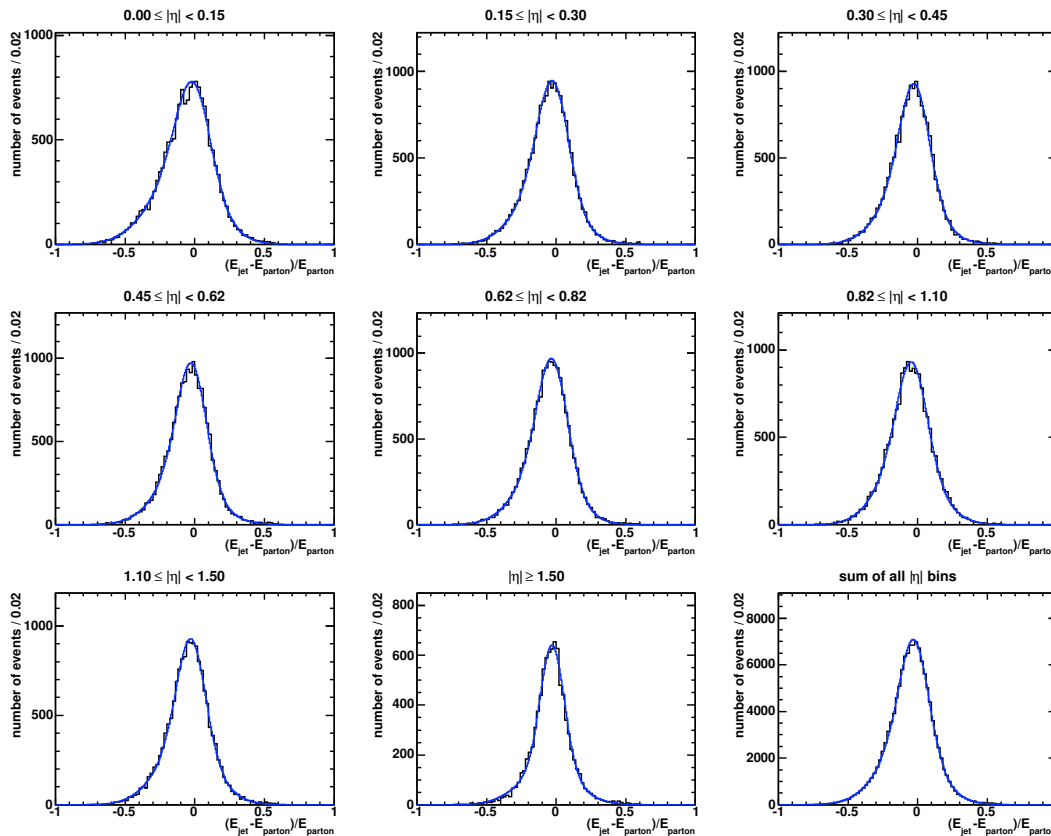


FIG. 2: Energy transfer functions for light quarks.

IV. METHOD VALIDATION AND CALIBRATION

The method validation checks the accuracy and consistency of the measured quantities. We observe shifts in the residual mass as we move from ideal to more realistic event sample composition (Table IV) which we must correct for in our method calibration. We perform a series of linearity tests based on pseudo-experiments using Monte Carlo simulated events. The linearity tests check the response of the method to the three relevant input parameters: m_t , Δ_{JES} and input signal fraction f . If the residuals or pull widths display any dependence on any of those parameters, a calibration with respect to that parameter will be necessary.

PE Sample	Residual mean shift	
	$m_t, GeV/c^2$	Δ_{JES}
good events only	0.0 ± 0.1	-0.09 ± 0.02
good, but all comb	-0.6 ± 0.1	-0.04 ± 0.02
all signal	-0.8 ± 0.1	-0.23 ± 0.02
signal and background	-1.2 ± 0.1	-0.34 ± 0.02

First, we see that residuals and pulls are constant with respect to the input m_t . A set of linearity plots check the response to input Δ_{JES} (Figures 6 and 7). Both mass and Δ_{JES} residuals depend on input Δ_{JES} . We correct for it with the “ Δ_{JES} calibration functions” as follows:

$$\Delta_{JES}^{\Delta_{JES} \text{ corrected}} = \frac{\Delta_{JES}^{\text{measured}} + 0.351}{1 - 0.148} \quad (7)$$

$$m_t^{\Delta_{JES} \text{ corrected}} = m_t^{\text{measured}} + 1.152 - 0.384 \Delta_{JES}^{\Delta_{JES} \text{ corrected}} \quad (8)$$

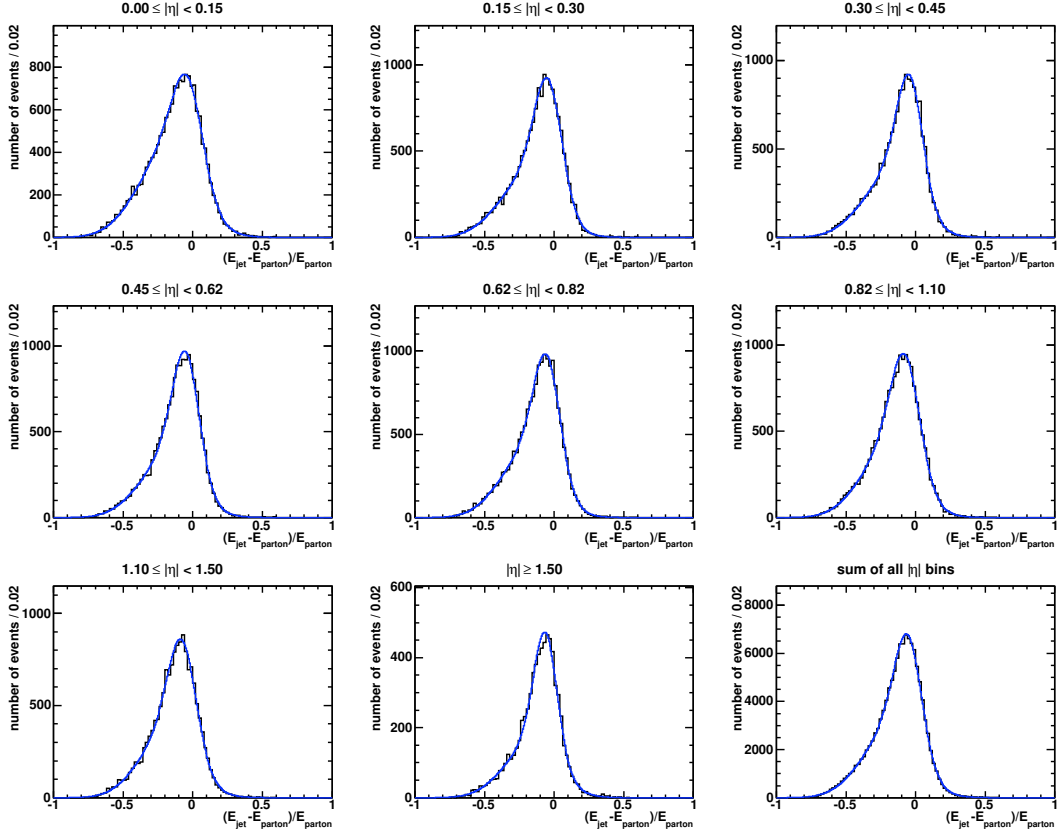


FIG. 3: Energy transfer functions for b-quarks.

The performance of the calibration functions can be tested by re-running the PEs with the calibration in place. The results are shown in Figures 8 and 9. The correction removes the dependence on input Δ_{JES} .

The final test is the dependence on input signal fraction f . Note that the signal fraction calibration is performed after the Δ_{JES} calibration, and so the PEs used in the following plots were all corrected using Equations 7 and 8. Both the residuals and pull widths show a strong dependence on f . This is expected, as the bias caused by background events naturally increases as f is decreased. Figures 10 and 11 show the dependence of the measured quantities on f .

However, our method does not measure f , but it is strongly correlated with measured ν_{sig} . We therefore parameterize the calibration with respect to measured ν_{sig} (Figures 12 and 13):

$$\begin{aligned}
 m_t^{final} &= m_t^{\Delta_{JES} \text{ corrected}} + 5.940 - 14.083 \nu_{sig} + 7.662 \nu_{sig}^2 \\
 \sigma_{m_t}^{final} &= s_m \sigma_{m_t}^{measured} \\
 s_m &= 1.829 - 1.575 \nu_{sig} + 1.061 \nu_{sig}^2
 \end{aligned} \tag{9}$$

$$\begin{aligned}
 \Delta_{JES}^{final} &= \Delta_{JES}^{\Delta_{JES} \text{ corrected}} + 1.426 - 3.337 \nu_{sig} + 1.690 \nu_{sig}^2 \\
 \sigma_{\Delta_{JES}}^{final} &= s_J \sigma_{\Delta_{JES}}^{measured} \\
 s_J &= 1.976 - 1.771 \nu_{sig} + 1.222 \nu_{sig}^2
 \end{aligned} \tag{10}$$

Post-correction, the dependencies on f are removed. Just as with the “ Δ_{JES} correction”, the actual dependence of the residuals on the signal fraction has a small effect on the correction since the signal fraction varies only in the range from 0.6 to 0.8.

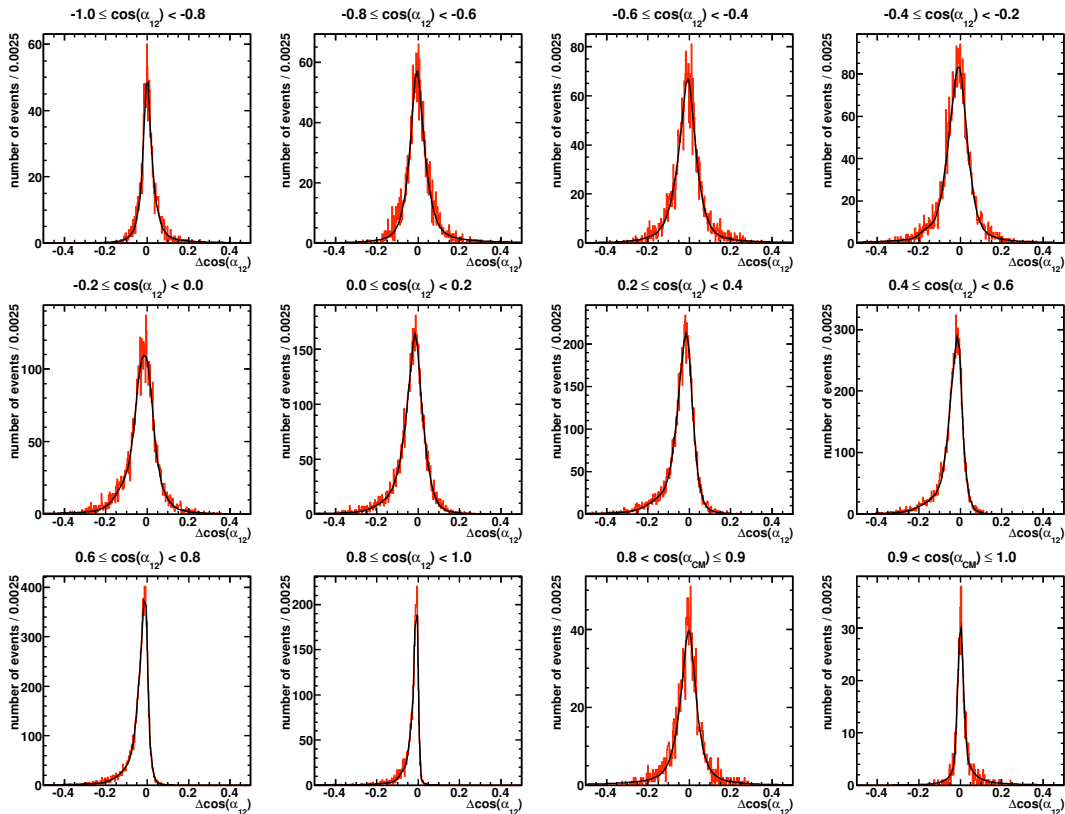


FIG. 4: Angular transfer functions parametrization for α_{12}

The mass and Δ_{JES} residuals along with the pull widths after all corrections, are shown in Figures 14 to 15. The errors are inflated according to the corrections (Equations 9 and 10) and Histogram in the Figure 16 shows an example of the distribution of statistical uncertainties expected for the mass measurement.

V. SYSTEMATIC UNCERTAINTIES

We evaluated the expected systematic uncertainties of our measurement technique and the results are summarized in Table II. Below we briefly summarize the standard procedures used for evaluating each systematic effect.

We evaluate our Monte Carlo generator uncertainty by comparing results obtained from 175 GeV/c^2 MC samples created with different MC generators (Pythia and Herwig). The jet energy scale residual systematic is measured by

TABLE II: Contributions to the total expected systematic uncertainty.

Systematics source	Expected contribution
MC Generator	0.70
Δ_{JES} Residual	0.65
Color Reconnection	0.56
B Jet	0.39
Background	0.37
ISR/FSR	0.24
Multiple Hadron Interaction	0.22
PDF	0.13
Lepton Energy	0.12
Calibration	0.12
Total	1.3

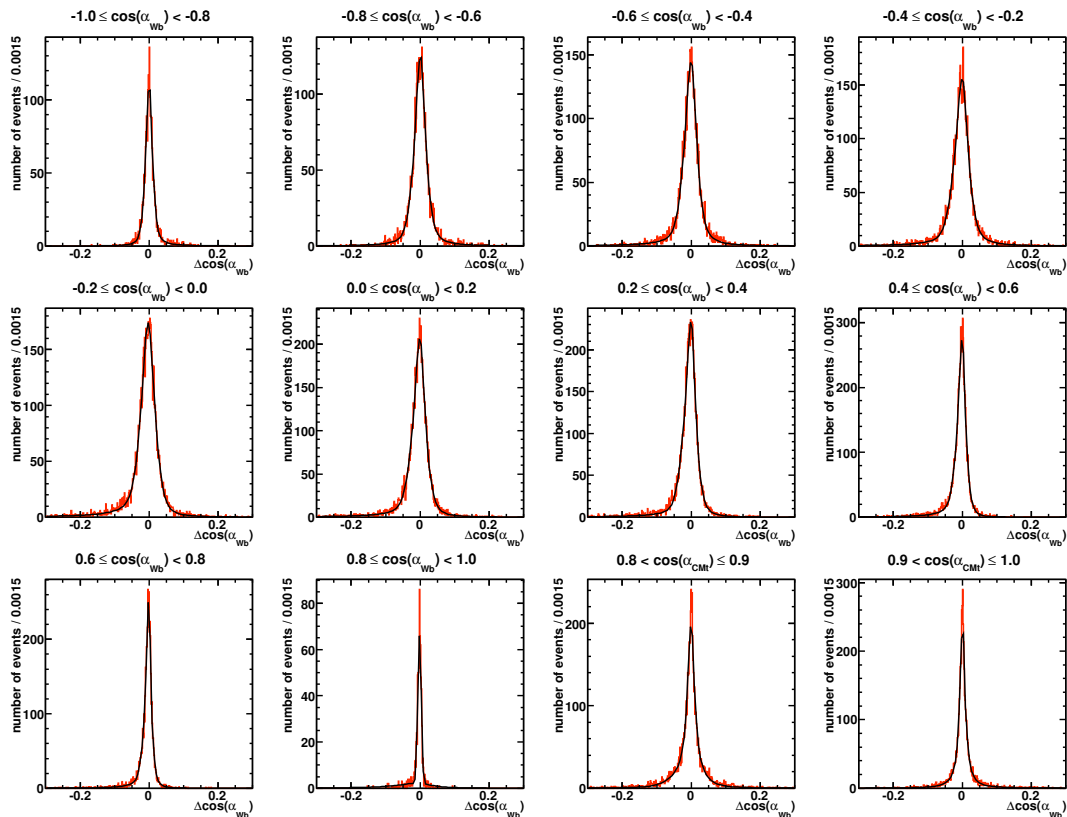


FIG. 5: Angular transfer functions parametrization for α_{Wb}

summing in quadrature the uncertainty resulting from each level of the CDF jet corrections. The color reconnection uncertainty is evaluated by comparing results from MC samples with and without color reconnection. The b jet systematic uncertainty is taken as the sum in quadrature of three separate uncertainties. First, we re-weight events to scale a 1 sigma shift in the semi-leptonic branching ratios. Next, we re-weight events to model different parameters in the fragmentation model. Finally, we measure the effect of a 1 sigma shift in the b jet energy scale. We evaluate our background systematic by measuring the shifts caused by using different signal fraction, relative contributions from each background source, and shapes from Q^2 values in our pseudo-experiments. Initial and final state radiation (ISR/FSR) uncertainty is estimated from MC samples with increased and decreased initial and final state radiation. The Multiple Hadron Interaction systematic is measured by re-weighting events to account for mismodeling of the luminosity profile and minbias events in our MC. The PDF uncertainty is taken as the sum in quadrature of three uncertainties. First, we look at the difference between two samples with different values for Λ_{QCD} . Next, we re-weight our events to scale the percentage of gluon-gluon fusion events up from 5% to 20%. At the end we re-weight our events based on 20 different pairs of CTEQ6M eigenvectors. The lepton energy systematic is taken as the sum in quadrature of the systematic uncertainties from a 1 sigma shift in lepton energy evaluated independently for electrons and muons. Finally, we evaluate our calibration uncertainty by varying our calibration functions within their 1 sigma uncertainties.

VI. THE MEASUREMENT

We use CDF dataset which includes all data collected between February 04 2002 and August 24 2008 and corresponds to an integrated luminosity of approximately $3.2 fb^{-1}$. Our selection procedure results in 578 candidate $t\bar{t}$ lepton+jets events and we measure

$$m_t = [172.4 \pm 1.4(stat + JES) \pm 1.3(syst)] GeV/c^2 = [172.4 \pm 1.9] GeV/c^2. \quad (11)$$

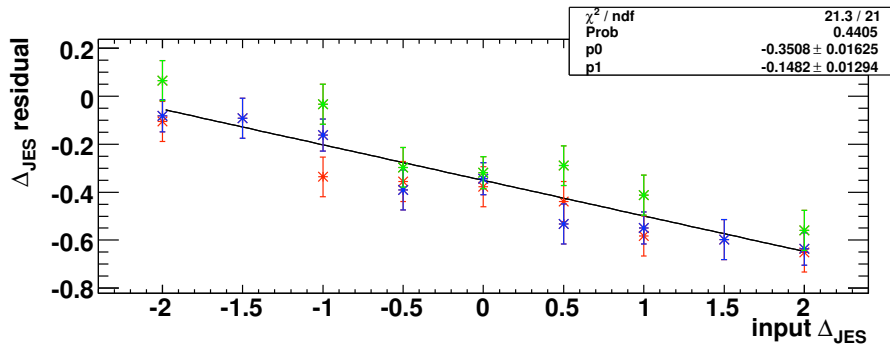


FIG. 6: Measured Δ_{JES} vs input Δ_{JES} . Colors show different top quark masses used in the simulation: 165(red), 175(green) and 185 GeV/c^2 (blue).

The corresponding values of Δ_{JES} and ν_{sig} , and their statistical uncertainties, are

$$\Delta_{JES} = 0.3 \pm 0.3, \quad (12)$$

$$\nu_{sig} = 0.63 \pm 0.03. \quad (13)$$

The log likelihood contours on Figure 16 show the result.

Acknowledgments

We thank the Fermilab staff and the technical staffs of the participating institutions for their vital contributions. This work was supported by the U.S. Department of Energy and National Science Foundation; the Italian Istituto Nazionale di Fisica Nucleare; the Ministry of Education, Culture, Sports, Science and Technology of Japan; the Natural Sciences and Engineering Research Council of Canada; the National Science Council of the Republic of China; the Swiss National Science Foundation; the A.P. Sloan Foundation; the Bundesministerium fuer Bildung und Forschung, Germany; the Korean Science and Engineering Foundation and the Korean Research Foundation; the Particle Physics and Astronomy Research Council and the Royal Society, UK; the Russian Foundation for Basic Research; the Comision Interministerial de Ciencia y Tecnologia, Spain; and in part by the European Community's Human Potential Programme under contract HPRN-CT-20002, Probe for New Physics.

-
- [1] Abulencia, A. and others, CDF, "Precise measurement of the top quark mass in the lepton+jets topology at CDF II", Phys. Rev. Lett. **99** (2007) 182002, hep-ex/0703045.
 - [2] F. Abe, et al., Nucl. Instrum. Methods Phys. Res. A **271**, 387 (1988); D. Amidei, et al., Nucl. Instrum. Methods Phys. Res. A **350**, 73 (1994); F. Abe, et al., Phys. Rev. D **52**, 4784 (1995); P. Azzi, et al., Nucl. Instrum. Methods Phys. Res. A **360**, 137 (1995); The CDFII Detector Technical Design Report, Fermilab-Pub-96/390-E
 - [3] T. Sjostrand et al., High-Energy-Physics Event Generation with PYTHIA 6.1, Comput. Phys. Commun. **135**, 238 (2001).
 - [4] G. Corcella et al., HERWIG 6: An Event Generator for Hadron Emission Reactions with Interfering Gluons (including supersymmetric processes), JHEP **01**, 10 (2001).
 - [5] F. James and M. Roos, Comput. Phys. Commun. **10**, 343 (1975).
-

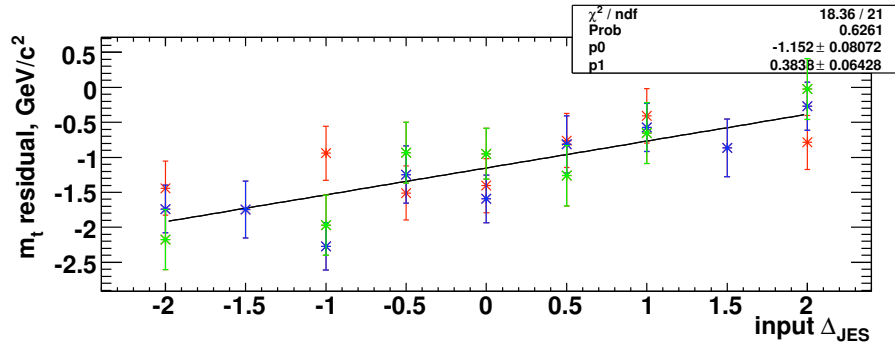


FIG. 7: Measured m_t vs input Δ_{JES} . Colors show different top quark masses used in the simulation: 165(red), 175(green) and 185 GeV/c^2 (blue).

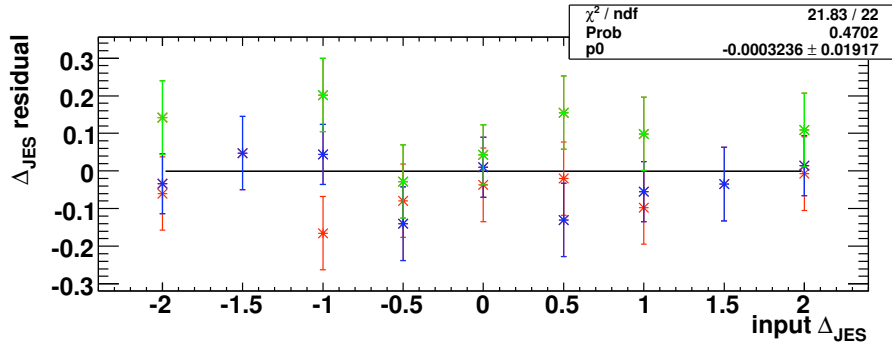


FIG. 8: Measured Δ_{JES} vs input Δ_{JES} , after the Δ_{JES} calibration.

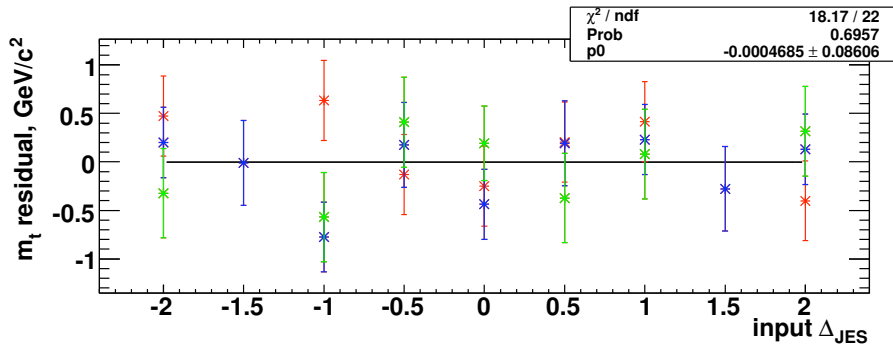


FIG. 9: Measured m_t vs input Δ_{JES} , after the Δ_{JES} calibration.

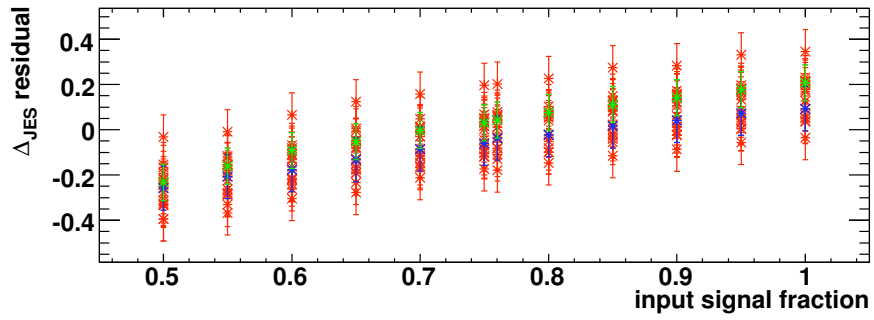


FIG. 10: Measured Δ_{JES} vs input signal fraction f . Colors show different top quark masses used in the simulation: 165 (green) and 185 GeV/c^2 (blue), and many points in between (red).

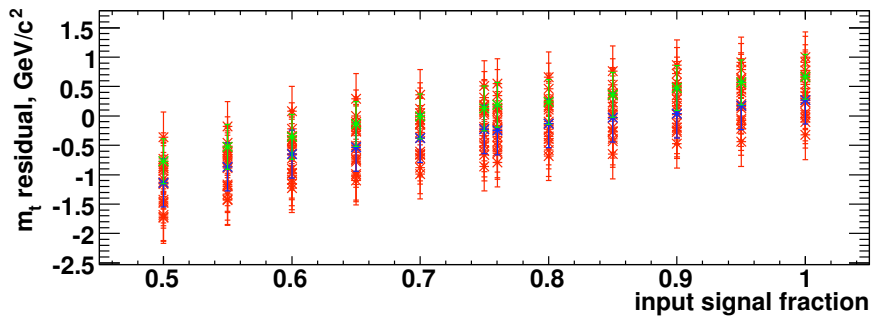


FIG. 11: Measured m_t vs input signal fraction f .

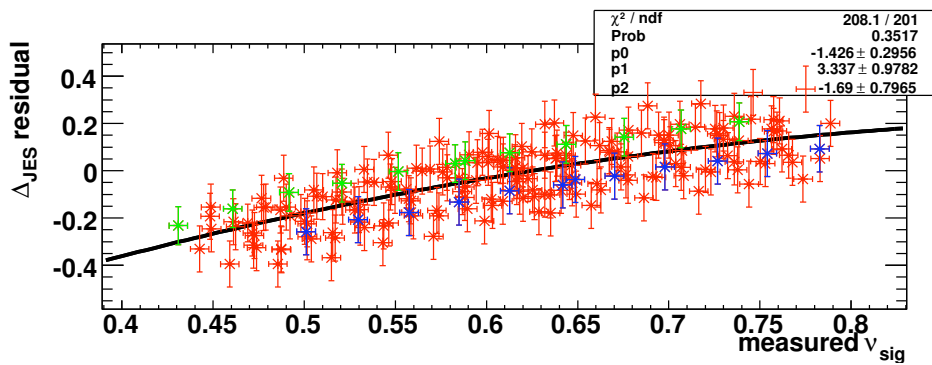
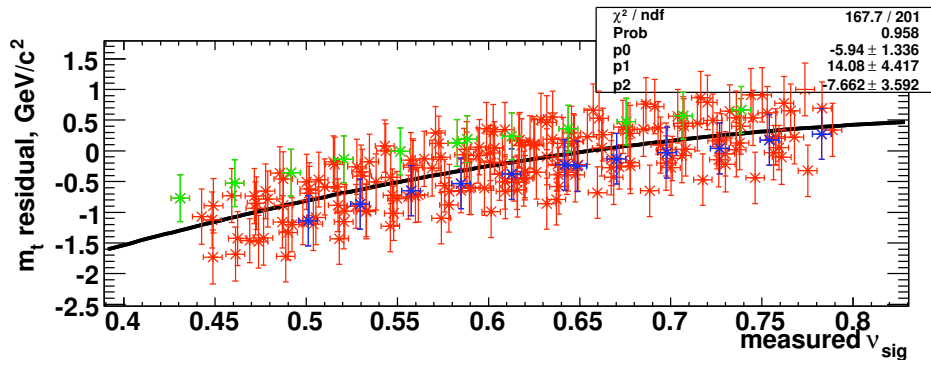
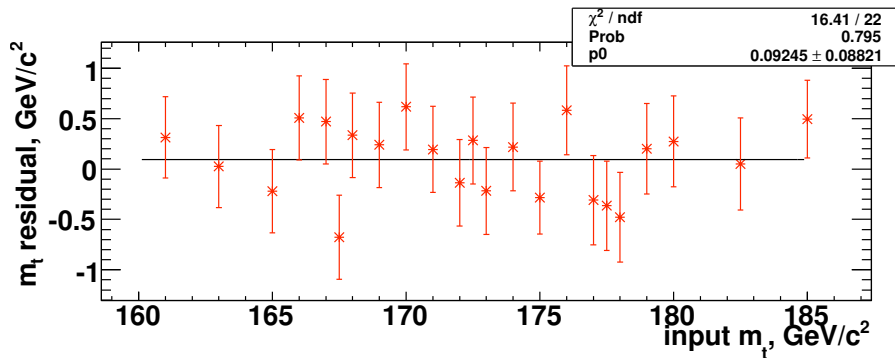
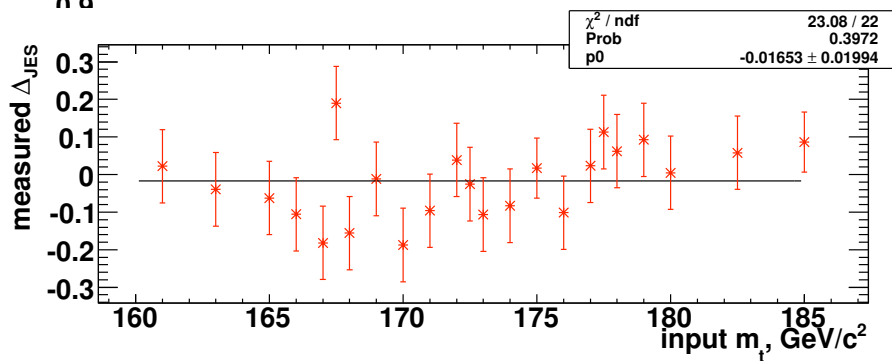


FIG. 12: Measured Δ_{JES} vs fitted v_{sig} .

FIG. 13: Measured m_t vs fitted ν_{sig} .FIG. 14: m_t residuals, after all corrections, versus input m_t FIG. 15: Δ_{JES} residuals, along with the mass pull widths and expected statistical uncertainties on m_t , after all corrections, versus input m_t .

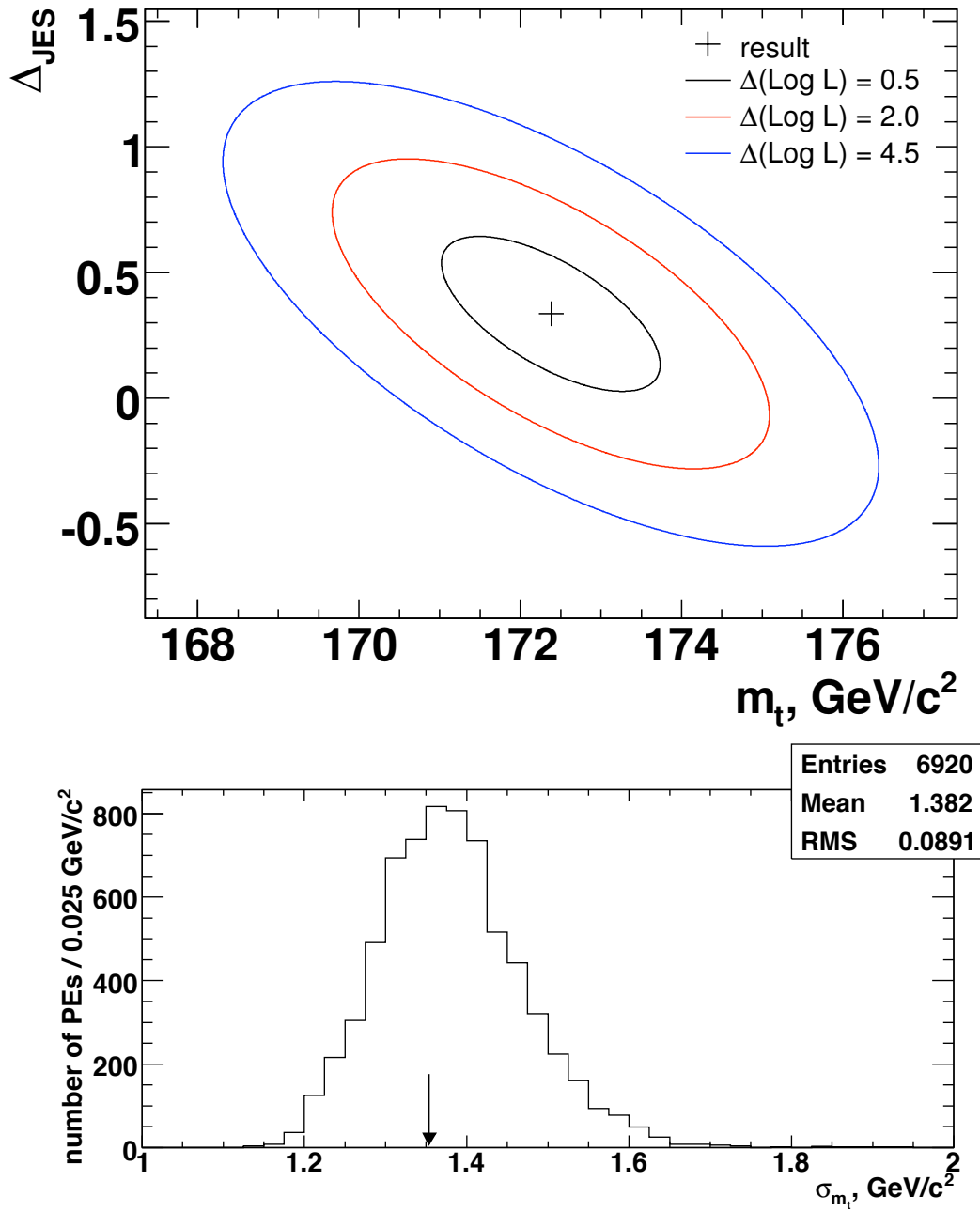
CDF Run II Preliminary, 3.2 fb⁻¹

FIG. 16: Contours of the log likelihood function for the data after calibration corrections, corresponding to the difference of 0.5, 2.0 and 4.5 from the maximum value (top); and the m_t statistical error measured in data (arrow) with the distribution of expected error at $m_t = 172.5 \text{ GeV}/c^2$ (bottom).

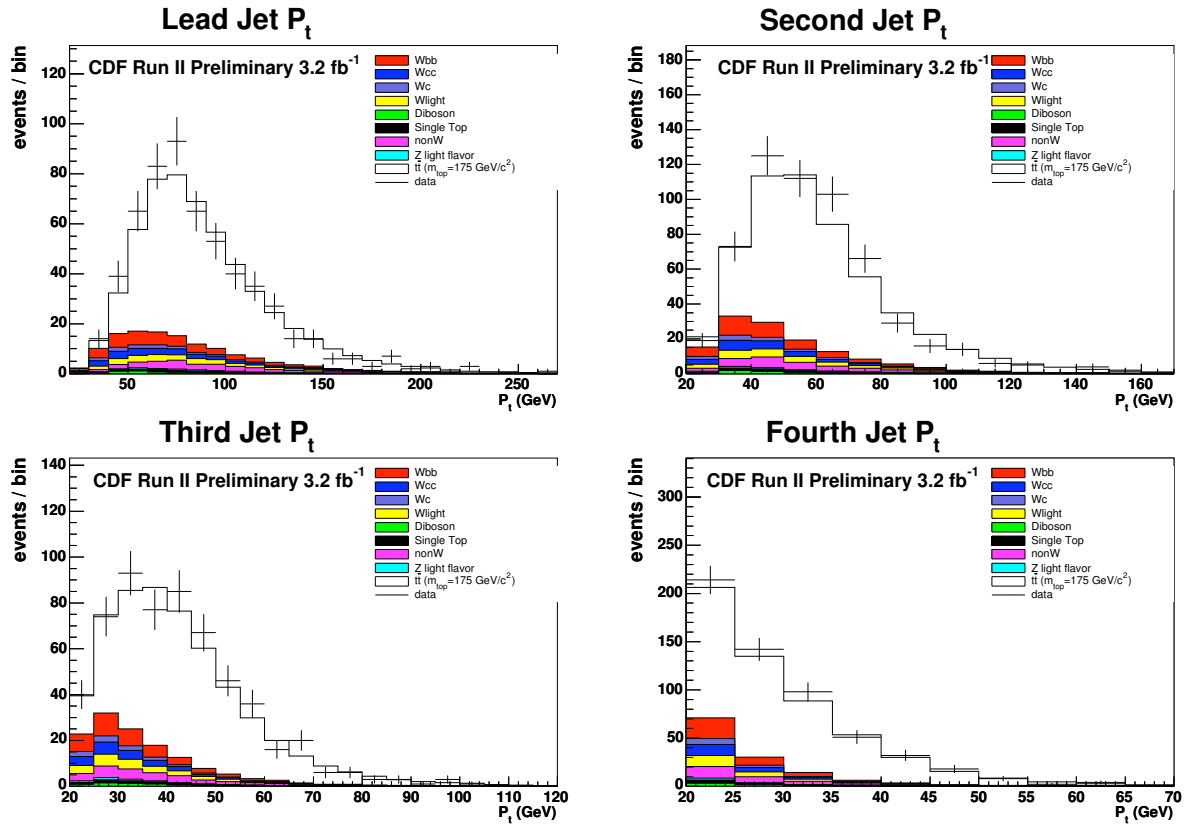


FIG. 17: Jet P_t ordered by jet energy. Stacked histograms are MC. Points are data.